 doi:10.20944/preprints201911.0280.v1

Article

Calculation of Maximum Total Supply Capacity of Three-Phase Unbalance Distribution Network Based on Mixed Integer Second-Order Cone

Jieyun Zheng [1], Shiyuan Ni [1], Pengjia Shi [1], Guilian Wu [1], Ri'an Wang [2,*], Chenying Yi [2] and Zhijian Hu [2]

[1] State Grid Fujian Economic Research Institute, Fuzhou 350000, China;
[2] School of Electrical Engineering and Automation, Wuhan University, Wuhan 430072, China;
zjy_0701@163.com (J.Z.); shiyuan_ni@whu.edu.cn (S.N.); shipengjia@zju.edu.cn (P.S.); wgltd@163.com (G.W.)
* Correspondence: wang546005065@163.com

Abstract: Considering the fault "N-1" checksum and the power flow, the single-phase power flow model is further transformed into a three-phase power flow model, and the asymmetry of the three-phase power flow is measured by the three-phase unbalance factor. The calculation model is linearized by the second-order cone relaxation and the Big-M method. At the same time, the load response and distribution network reconstruction are used to improve the reliability of the power supply network to cope with the power failure. The relationship between power supply capability and power flow constraints, main transformer capacity and distributed power parameters is analyzed by IEEE 33-node three-phase power distribution system. The feasibility of the proposed model and the accuracy of the second-order cone relaxation are verified by numerical examples, which provides a technical reference for distribution network planning.

Keywords: distribution network; total supply capacity; second-order cone relaxation; power flow calculation; load response; Big-M method; three-phase unbalance degree

---

1. Introduction

The total supply capacity (TSC) of distribution network refers to the maximum load supply capacity within a certain power supply range based on interconnections of main transformers when meeting the "N-1" guideline and actual operation constraints [1]. TSC characterizes the power supply reliability of distribution network, and the accurate calculation of it is conducive to the planning and refined load management of distribution network in line with the increasing load demand.

At present, the research on the calculation of power supply capacity has experienced three stages in its development process [2-3]. In the first stage, the power supply capacity was evaluated based on the substation capacity and capacity-load ratio. However, the effect of the subordinate network on the power supply capacity had not been considered at this stage, and the calculation results cannot reflect the power supply requirements precisely. The second stage is the initial stage that considered the substation capacity and the power transfer capability of network at the same time, but only the feeder load was taken into account in the evaluation of power transfer capability, which may lead to deviation. And the third stage is the precise theoretical modeling stage of power supply capacity [4], taking into account the "N-1" guideline, substation capacity and power transfer capability of network. Reference [5] proposed a calculation method of power supply capacity based on interconnections of main transformers and "N-1" guideline. Considering the two points that mentioned above, the calculation method of power supply capacity considering the contact capacity and the short-time overload problem of the main transformers was proposed in reference [6], which

Preprints (www.preprints.org) | NOT PEER-REVIEWED | Posted: 24 November 2019 doi:10.20944/preprints201911.0280.v1

can help to improve the accuracy of calculation results. Based on power flow calculation, reference [7] established an TSC model considering the voltage drop and network loss, which considers the interconnections between feeders and the "N-1" fault of main transformers and feeders at the same time. The model and the calculation method can be applied to the field of the operation in distribution network.

In recent years, with the development of smart grid and power distribution automation, the proportion of some equipment that access to distribution network has been increasing, such as distributed generation (DG) and flexible load, which has certain impact on the planning and operation of distribution network. This phenomenon should be considered in the calculation of power supply capacity, and some studies have considered the impact of the above factors in the calculation process. Taking the maximum expected value of the load amplification factor under the typical DG output scenario as the optimization goal, reference [8] established a calculation model of TSC, which considers the site selection of DG and network reconfiguration. The calculation results show that the access of DG is beneficial to the improvement of TSC. Reference [9] established a two-layer optimization model for TSC considering the uncertainty of DG output. In this model, the economic operation of the active distribution network is considered, but the "N-1" safety guideline is not included in the constraints. In reference [10], the TSC model including users grading and interaction between demand-side and grid was established. The load in demand-side response is considered as interruptible load and emergency load, and simulation of the paper shows that the interaction between users and grid can improve the TSC of distribution network. It can be seen from the above research status that both DG and flexible load can play a role in improving TSC, but few studies have considered the relationship between them in the calculation model of TSC.

One problem that should also be considered when calculate TSC is that after the equipment such as DG and flexible load are connected to the distribution network in phase, the original three-phase asymmetry of the distribution network will be more serious. If the single-phase equivalent model in the previous study is continuously used in the analysis of the TSC, the calculation results will be out of the actual situation of the distribution network and might also lead to a large deviation [11-13]. Therefore, the three-phase asymmetry of the distribution network must be fully considered.

In summary, based on the mixed integer second-order cone optimization method, the following solutions are proposed by combining the three-phase power flow calculation model proposed in [16]:

1. Fully consider the three-phase asymmetry of the distribution network, establish a mathematical model of each asymmetry factor, and accurately calculate the TSC of the distribution network through the three-phase power flow calculation method and the simulation of "N-1" fault.
2. Use the distribution network reconfiguration model to enhance the flexibility of TSC, and transform the nonlinear model established by the Big-M method into a mixed integer model according to the method of [20]. At the same time, based on the actual situation, set the minimum load demand for all load nodes and add part of the unimportant load into the regulation range of load response.

Through the simulation of the improved IEEE 33-node three-phase distribution system, the effectiveness of the proposed model and scheme was confirmed.

2. Three-Phase Power Flow Model

According to Kirchhoff's law, the sum of the power that flowing into the node is equal to the sum of outflows in distribution network. Therefore, for any node j, the three-phase active and reactive power can be described as:

$$\begin{cases} \sum P_j^{\varphi} = P_j^{\varphi} + P_{j,\mathrm{DG}}^{\varphi} + P_{j,\mathrm{T}}^{\varphi} \\ \sum Q_j^{\varphi} = Q_j^{\varphi} + Q_{j,\mathrm{DG}}^{\varphi} + Q_{j,\mathrm{T}}^{\varphi} \end{cases} \tag{1}$$

- $\varphi \in \{\mathrm{A, B, C}\}$ refers to phase A, B and C;

Preprints (www.preprints.org) | NOT PEER-REVIEWED | Posted: 24 November 2019 doi:10.20944/preprints201911.0280.v1

- P_j^{φ} and Q_j^{φ} refer to the three-phase active power and reactive power of the load demand at node j, respectively;
- $\sum P_j^{\varphi}$ and $\sum Q_j^{\varphi}$ refer to the net injection quantities of three-phase active and reactive power, respectively;
- $P_{j,\mathrm{DG}}^{\varphi}$ and $Q_{j,\mathrm{DG}}^{\varphi}$ refer to the three-phase active power and reactive power of the DG at node j, respectively;
- $P_{j,\mathrm{T}}^{\varphi}$ and $Q_{j,\mathrm{T}}^{\varphi}$ refer to the three-phase active and reactive power input by the substation to node j, respectively.

For the radial distribution network, the power flow formulas in the form of distflow [14] can be described as shown in formula (2).

$$\begin{cases} \sum\limits_{i\in u(j)} \left(P_{ij}^{\varphi} - (I_{ij}^{\varphi})^2 r_{ij}^{\varphi}\right) + \sum P_j^{\varphi} = \sum\limits_{k\in v(j)} P_{jk}^{\varphi} \\ \sum\limits_{i\in u(j)} \left(Q_{ij}^{\varphi} - (I_{ij}^{\varphi})^2 x_{ij}^{\varphi}\right) + \sum Q_j^{\varphi} = \sum\limits_{k\in v(j)} Q_{jk}^{\varphi} \\ (V_j^{\varphi})^2 = (V_i^{\varphi})^2 - 2(r_{ij}^{\varphi} P_{ij}^{\varphi} + x_{ij}^{\varphi} Q_{ij}^{\varphi}) + ((r_{ij}^{\varphi})^2 + (x_{ij}^{\varphi})^2)\cdot(I_{ij}^{\varphi})^2 \end{cases} \tag{2}$$

- $u(j)$ refers to the set of the head nodes of branches with j as the end node in the distribution system;
- $v(j)$ refers to the set of the end nodes of branches with j as the head node;
- P_{ij}^{φ} and Q_{ij}^{φ} refer to the three-phase active and reactive power flowing on branch ij, respectively;
- r_{ij}^{φ} and x_{ij}^{φ} refer to the three-phase resistance and reactance of branch ij, respectively;
- P_{jk}^{φ} and Q_{jk}^{φ} refer to the three-phase active and reactive power flowing on branch jk, respectively;
- V_i^{φ} and V_j^{φ} refer to the three-phase voltage amplitudes of node i and node j, respectively;

The second-order cone relaxation I_{ij}^{φ} is the current amplitude of branch ij, which can be calculated by formula (3).

$$(I_{ij}^{\varphi})^2 = \frac{(P_{ij}^{\varphi})^2 + (Q_{ij}^{\varphi})^2}{(V_i^{\varphi})^2} \tag{3}$$

There are some non-convex terms such as quadratic terms and negative quadratic terms in the power flow formulas that mentioned above, which will make the optimization problem with power flow constraints difficult to solve. The solution methods of this problem mainly include seeking local optimal solutions, approximate linearization and convex relaxation for power flow constraints [14-15]. Among those methods, the convex relaxation technique is widely applied to ensure the efficiency of the algorithm and the optimality of the solution. Therefore, for the above-mentioned power flow formulas, the second-order cone programming (SOCP) method has good applicability [16]. Replace the variables in formula (2) and formula (3) as follows:

$$\begin{cases} v_{2,j}^{\varphi} = (V_j^{\varphi})^2 \\ i_{2,ij}^{\varphi} = (I_{ij}^{\varphi})^2 = \dfrac{(P_{ij}^{\varphi})^2 + (Q_{ij}^{\varphi})^2}{v_{2,i}^{\varphi}} \end{cases} \tag{4}$$

The second term in formula (4) can be further relaxed and converted into a standard second-order cone type:

$$\left\| [2P_{ij}^{\varphi} \quad 2Q_{ij}^{\varphi} \quad i_{2,ij}^{\varphi} - v_{2,i}^{\varphi}]^{\mathrm{T}} \right\|_2 \le i_{2,ij}^{\varphi} + v_{2,i}^{\varphi} \tag{5}$$

The final SOCP form of the power flow formulas can be described as:

Preprints (www.preprints.org) | NOT PEER-REVIEWED | Posted: 24 November 2019 doi:10.20944/preprints201911.0280.v1

$$\begin{cases} \sum_{i\in u(j)} \left(P_{ij}^{\varphi} - i_{2,ij}^{\varphi} r_{ij}^{\varphi}\right) + \sum P_{j}^{\varphi} = \sum_{k\in v(j)} P_{jk}^{\varphi} \\ \sum_{i\in u(j)} \left(Q_{ij}^{\varphi} - i_{2,ij}^{\varphi} x_{ij}^{\varphi}\right) + \sum Q_{j}^{\varphi} = \sum_{k\in v(j)} Q_{jk}^{\varphi} \\ v_{2,j}^{\varphi} = v_{2,i}^{\varphi} - 2(r_{ij}^{\varphi} P_{ij}^{\varphi} + x_{ij}^{\varphi} Q_{ij}^{\varphi}) + ((r_{ij}^{\varphi})^2 + (x_{ij}^{\varphi})^2) i_{2,ij}^{\varphi} \\ \left\| [2P_{ij}^{\varphi} \quad 2Q_{ij}^{\varphi} \quad i_{2,ij}^{\varphi} - v_{2,i}^{\varphi}]^{\mathrm{T}} \right\|_2 \le i_{2,ij}^{\varphi} + v_{2,i}^{\varphi} \end{cases} \tag{6}$$

3. Factors Affecting Three-Phase Asymmetry of Distribution Network

Distribution network contains a large number of asymmetric lines and loads, which makes it possess the characteristic of three-phase asymmetric. After the flexible load and the DG that operate in a non-full-phase state connected to the distribution network, the asymmetry characteristic appears to be more significant. In the above situation, if the traditional single-phase equivalent model is still used in the analysis, a large error will result. Therefore, in order to comprehensively evaluate the power demand of users and accurately calculate the TSC of distribution network, it is necessary to analyze the typical factors of three-phase asymmetry and introduce the concept of three-phase unbalance factor to describe the unbalance degree of distribution network.

3.1. Three-phase Asymmetric Load

The asymmetry of three-phase load is the main cause of three-phase unbalance in power system. The asymmetry of load mainly comes from the uneven distribution of single-phase load of power users in the system [17]. When calculating the TSC of distribution network, the equivalent of a three-phase load to a single-phase model will not accurately assess the actual demand of each phase load, so the load conditions of each phase should be considered separately.

3.2. Three-phase Asymmetric DG

When a single-phase DG (such as single-phase photovoltaic generator, single-phase wind turbine, etc.) is connected in distribution network, the output of each phase is usually not completely equal due to the uncontrollable factors such as geography and climate, which will make the distribution network that is originally not a fully one more asymmetrical [18]. When analyzing a distribution network containing DG, the influence of DG on the three-phase unbalance should be fully considered. This paper refers to [16] to equivalently treat the DG into PQ types.

3.3. Three-Phase Unbalance Factor of Node Voltage

The degree of three-phase asymmetry of distribution network is described by the voltage unbalance factor, which can be described as follows [19]:

$$\lambda_i^{\varphi} = \frac{\left|V_i^{\varphi} - V_i^{\mathrm{avg}}\right|}{V_i^{\mathrm{avg}}} \tag{7}$$

- V_i^{φ} refers to the voltage amplitude of phase φ;
- V_i^{avg} refers to the average value of the three-phase voltage amplitude.

In Section 2, the node voltage amplitude can be replaced according to formula (4), and the following formula can be obtained:

$$\begin{cases} \lambda_{2,i}^{\varphi} = \dfrac{\left|v_{2,i}^{\varphi} - v_{2,i}^{\mathrm{avg}}\right|}{v_{2,i}^{\mathrm{avg}}} \\ v_{2,i}^{\mathrm{avg}} = \dfrac{\sum v_{2,i}^{\varphi}}{3} \end{cases} \tag{8}$$

Define ε as the maximum value of voltage unbalance factor. When the condition $\lambda_{2,i}^{\varphi} \ge \varepsilon$ is satisfied, the condition $\lambda_i^{\varphi} \ge \varepsilon$ must also be satisfied. The specific derivation process is shown in the

Preprints (www.preprints.org) | NOT PEER-REVIEWED | Posted: 24 November 2019 doi:10.20944/preprints201911.0280.v1

Appendix. Therefore, the variables in the voltage unbalance factor can be replaced by the relaxed variables in the SOCP-type power flow formulas, as shown in the first term of formula (8).

4. Calculation Model of TSC

4.1. Objective Function

The objective is given by

$$Max\left|\sum_{\varphi}\sum_{i\in\Phi_B} P_i^{\varphi}\right| \tag{9}$$

$$Max\left|\left(\sum_{\varphi}\sum_{i\in\Phi_B} P_i^{\varphi} + \phi\sum_{n}\sum_{\varphi}\sum_{ij} I_{2,ij}^{\varphi,t(n)} r_{ij}\right)\right| \tag{10}$$

- P_i^{φ} refers to the active load demand;
- Φ_B refers to the set of all nodes;
- ϕ refers to the weight of the loss factor in the objective function.

The meanings of the formulas are as follows:

- Equation (9) refers to the maximum active load supplied by the entire distribution network.
- In order to consider the influence of network loss on the power supply capacity and minimize it, the formula (9) is converted into the formula (10).

The "N-1" guideline means that when any power supply component fails alone, the system continues to supply power to the original load. It should be noted that the line fault has less impact on the TSC than the substation fault. Therefore, only the substation to perform "N-1" needs to be verified.

4.2. Constraints

$$I_{2,ij}^{\varphi,t(\mathrm{n})} = (I_{ij}^{\varphi,t(\mathrm{n})})^2 \tag{11}$$

$$\sum_{i\in u(j)}\left(P_{ij}^{\varphi,t(\mathrm{n})} - I_{2,ij}^{\varphi,t(\mathrm{n})} r_{ij}^{\varphi}\right) + \sum P_j^{\varphi,t(\mathrm{n})} = \sum_{k\in v(j)} P_{jk}^{\varphi,t(\mathrm{n})} \tag{12}$$

$$\sum P_j^{\varphi,t(\mathrm{n})} = P_j^{\varphi} + P_{j,DG}^{\varphi,t(\mathrm{n})} + P_{j,\mathrm{T}}^{\varphi,t(\mathrm{n})} \tag{13}$$

$$\sum_{i\in u(j)}\left(Q_{ij}^{\varphi,t(\mathrm{n})} - I_{2,ij}^{\varphi,t(\mathrm{n})} x_{ij}^{\varphi}\right) + \sum Q_j^{\varphi,t(\mathrm{n})} = \sum_{k\in v(j)} Q_{jk}^{\varphi,t(\mathrm{n})} \tag{14}$$

$$\sum Q_j^{\varphi,t(\mathrm{n})} = Q_j^{\varphi} + Q_{j,DG}^{\varphi,t(\mathrm{n})} + Q_{j,\mathrm{T}}^{\varphi,t(\mathrm{n})} \tag{15}$$

- $I_{2,ij}^{\varphi,t(\mathrm{n})}$ refers to the current squared term of line ij. Use this auxiliary variable instead of the quadratic term to eliminate the nonlinear variables;
- $n(n=1,2,3,\cdots N_{trans})$ refers to the serial number of the substation, and N_{trans} refers to the total number of substations;
- $t(\mathrm{n})$ refers to the node number corresponding to the substation n;
- $P_{j,DG}^{\varphi,t(\mathrm{n})}$ and $Q_{j,DG}^{\varphi,t(\mathrm{n})}$ refer to the active and reactive input power of DG at node j, respectively;
- $P_{j,\mathrm{T}}^{\varphi,t(\mathrm{n})}$ and $\sum Q_j^{\varphi,t(\mathrm{n})}$ refer to the active and reactive input power of the substation at node j, respectively.

Equations (12) - (15) are the balance constraints of active and reactive power at nodes in power flow constraints. The balance formula of the power at node consists of three parts: the first part is the power flow of line ij, the second part is the power flow of line jk, and the last part is the node input power flow. It should be noted that in the case of failures of each substation, the load of the node is constant.

$$P_j^{\varphi} \le 0, Q_j^{\varphi} \le 0 \tag{16}$$

$$P_{j,DG}^{\varphi,t(\mathrm{n})} \ge 0, Q_{j,DG}^{\varphi,t(\mathrm{n})} \ge 0 \tag{17}$$

Preprints (www.preprints.org) | NOT PEER-REVIEWED | Posted: 24 November 2019 doi:10.20944/preprints201911.0280.v1

$$P_{j,\mathrm{T}}^{\varphi,t(\mathrm{n})} \geq 0, Q_{j,\mathrm{T}}^{\varphi,t(\mathrm{n})} \geq 0 \tag{18}$$

Equations (16) - (18) represents the flow direction of power. The symbol is positive when the power flows to, and it is negative when the power flows out the node.

$$V_{2,j}^{\varphi,t(\mathrm{n})} = (V_j^{\varphi,t(\mathrm{n})})^2 \tag{19}$$

$$V_{2,j}^{\varphi,t(\mathrm{n})} = V_{2,i}^{\varphi,t(\mathrm{n})} - 2(r_{ij}^{\varphi} P_{ij}^{\varphi,t(\mathrm{n})} + x_{ij}^{\varphi} Q_{ij}^{\varphi,t(\mathrm{n})}) + ((r_{ij}^{\varphi})^2 + (x_{ij}^{\varphi})^2) I_{2,ij}^{\varphi,t(\mathrm{n})} \tag{20}$$

$$I_{2,ij}^{\varphi,t(\mathrm{n})} = \frac{\left[(P_{ij}^{\varphi,t(\mathrm{n})})^2 + (Q_{ij}^{\varphi,t(\mathrm{n})})^2\right]^2}{V_{2,i}^{\varphi,t(\mathrm{n})}} \tag{21}$$

$$\left\| [2P_{ij}^{\varphi,t(\mathrm{n})} \quad 2Q_{ij}^{\varphi,t(\mathrm{n})} \quad I_{2,ij}^{\varphi,t(\mathrm{n})} - V_{2,i}^{\varphi,t(\mathrm{n})}]^{\mathrm{T}} \right\|_2 \leq I_{2,ij}^{\varphi,t(\mathrm{n})} + V_{2,i}^{\varphi,t(\mathrm{n})} \tag{22}$$

- $V_{2,j}^{\varphi,t(\mathrm{n})}$ replaces the quadratic term of $V_j^{\varphi,t(\mathrm{n})}$.

According to the power flow constraints for branch in the form of distflow, the branch should satisfy equations (20) - (21). According to the form of the second-order cone, the formula (21) can be deformed into the formula (22).

$$V_{i\in\Phi_T}^{\varphi,t(\mathrm{n})} = V_{base} \tag{23}$$

$$(V_i^{\varphi,\min})^2 \leq V_{2,i}^{\varphi,t(\mathrm{n})} \leq (V_i^{\varphi,\max})^2 \tag{24}$$

$$0 \leq I_{2,ij}^{\varphi,t(\mathrm{n})} \leq (I_{ij}^{\varphi,\max})^2 \tag{25}$$

$$\left| P_{j,\mathrm{T}}^{\varphi,t(\mathrm{n})} + Q_{j,\mathrm{T}}^{\varphi,t(\mathrm{n})} \right| \leq S_T \tag{26}$$

- $V_i^{\varphi,\max}$ and $V_i^{\varphi,\min}$ refer to the maximum voltage limit and minimum voltage limit of node i, respectively;
- $I_{ij}^{\varphi,\max}$ refers to the maximum allowable current of branch ij;
- S_T refers to the maximum capacity of the substation;
- V_{base} refers to the reference voltage of the distribution network.

In the formulas that mentioned above, formula (24) indicates the range of voltage values for all nodes; formula (25) indicates the range of current values for all branches; formula (26) indicates the capacity of the substation.

$$P_{i,T}^{\varphi,t(n)} = 0, i = t(n) \tag{27}$$

$$Q_{i,T}^{\varphi,t(n)} = 0, i = t(n) \tag{28}$$

Equation (27) and equation (28) indicate that when a substation fails, the substation of the corresponding node has no input power.

$$0 \leq I_{2,ij}^{\varphi,t(\mathrm{n})} \leq S_{ij}^{\varphi} M,\ S_{ij}^{\varphi} \in \{0,1\},\ j \in \Phi_S \tag{29}$$

$$V_{2,j}^{\varphi} \geq -M(1 - S_{ij}^{\varphi}) + V_{2,i}^{\varphi} - 2(r_{ij}^{\varphi} P_{ij}^{\varphi,t(\mathrm{n})} + x_{ij}^{\varphi} Q_{ij}^{\varphi,t(\mathrm{n})}) + ((r_{ij}^{\varphi})^2 + (x_{ij}^{\varphi})^2) I_{2,ij}^{\varphi,t(\mathrm{n})} \tag{30}$$

$$V_{2,j}^{\varphi} \leq M(1 - S_{ij}^{\varphi}) + V_{2,i}^{\varphi} - 2(r_{ij}^{\varphi} P_{ij}^{\varphi,t(\mathrm{n})} + x_{ij}^{\varphi} Q_{ij}^{\varphi,t(\mathrm{n})}) + ((r_{ij}^{\varphi})^2 + (x_{ij}^{\varphi})^2) I_{2,ij}^{\varphi,t(\mathrm{n})} \tag{31}$$

- S_{ij}^{φ} refers to the state of the circuit breaker on the line. When $S_{ij}^{\varphi} = 0$, it indicates that the circuit breaker is open, and when $S_{ij}^{\varphi} = 1$, the circuit breaker is in the connected state.
- M refers to a large enough value.

Equation (29) is processed by Big-M method, which can transform nonlinear problems into mixed integer linear programming. When the circuit breaker is disconnected, equation (20) is no longer applicable. Equations (30) and (31) transform the equation relationship into two inequality relations. When $S_{ij}^{\varphi} = 1$, the two inequalities are equivalent to the original constraint (20); when $S_{ij}^{\varphi} = 0$, as long as M is sufficiently large, there is no limit between the voltages across the line.

$$\sigma_{i\in\Phi_B}^{\varphi} \in \{0,1\},\ \sum \sigma_{i\in\Phi_B}^{\varphi} = N_{\sigma,\max} \tag{32}$$

Preprints (www.preprints.org) | NOT PEER-REVIEWED | Posted: 24 November 2019 doi:10.20944/preprints201911.0280.v1

$$\sigma_{i\in\Phi_B}^{\varphi} P_{i,DG}^{\varphi,\min} \le P_{i\in\Phi_B,DG}^{\varphi,t(n)} \le \sigma_{i\in\Phi_B}^{\varphi} P_{i,DG}^{\varphi,\max} \tag{33}$$

$$\sigma_{i\in\Phi_B}^{\varphi} Q_{i,DG}^{\varphi,\min} \le Q_{i\in\Phi_B,DG}^{\varphi,t(n)} \le \sigma_{i\in\Phi_B}^{\varphi} Q_{i,DG}^{\varphi,\max} \tag{34}$$

- $\sigma_{i\in\Phi_B}^{\varphi}$ refers to the investment decision variable of DG. When $\sigma_{i\in\Phi_B}^{\varphi}=1$, it indicates that DG is access to the node.
- $N_{\sigma,\max}$ refers to the total number of DG invested.

The input power of the DG is also processed by Big-M, as shown in equations (33) and (34).

$$\lambda_i^{A,t(n)} = \left|V_{2,i}^{A,t(n)} - V_{2,i}^{avg,t(n)}\right| \tag{35}$$

$$\lambda_i^{B,t(n)} = \left|V_{2,i}^{B,t(n)} - V_{2,i}^{avg,t(n)}\right| \tag{36}$$

$$\lambda_i^{C,t(n)} = \left|V_{2,i}^{C,t(n)} - V_{2,i}^{avg,t(n)}\right| \tag{37}$$

$$V_{2,i}^{avg,t(n)} = \frac{V_{2,i}^{A,t(n)} + V_{2,i}^{B,t(n)} + V_{2,i}^{C,t(n)}}{3} \tag{38}$$

$$\text{Max}(\lambda_i^{A,t(n)}, \lambda_i^{B,t(n)}, \lambda_i^{C,t(n)}) \le \lambda_{\max} \tag{39}$$

- $\lambda_i^{A,t(n)}$, $\lambda_i^{B,t(n)}$ and $\lambda_i^{C,t(n)}$ refer to the voltage unbalance factor of each phase of the node;
- $V_{2,i}^{avg,t(n)}$ refers to the upper limit of the unbalanced factor.

In the above formulas, equations (35) - (38) refer to the calculation process of three-phase unbalance; formula (39) means that the imbalance of the voltages of the respective phases cannot exceed the allowable upper limit.

$$P_j^{\varphi} \le -\lambda_j P_{j,need}^{\varphi} \tag{40}$$

- λ_j refers to the proportion of load demand reduction, and the value of it ranges from 0 to 1.

5. Simulation and Analysis

The simulation is programmed by the MATLAB platform and the Cplex solver in the Yalmip platform is used for optimization. The development environment is MATLAB R2014a. The test system's processor parameters are Intel(R) Core(TM) i5-4200H CPU clocked at 2.8GHz, memory is 4GB, and the operating system is Windows7 64bit.

Take the IEEE 33-node three-phase asymmetric power distribution system as example. The specific line parameters and the minimum load demand of each load node are detailed in [22]. The reference voltage of this system is 12.66 kV, and the lower limit of the node voltage is 0.9 p.u. The maximum capacity of the substation is 7 MVA, the maximum allowable current of the feeder line is 0.7 kA, the upper and lower limits of the distributed output are 0.1 MVA and 1 MVA, respectively, and the circuit breaker access positions are line 2-3 and line 4-5. The three-phase unbalance is allowed to be 10^{-3}.

In a traditional distribution network, a single power supply generally supplies power to all loads. When a power supply fails, all load nodes will face a significant risk of power outage. Therefore, the distribution network with high reliability requirements generally uses dual power supply or multiple power supply for important loads. When a single substation fails or is overhauled, the load facing the risk of power outage can be transferred to other substations to improve the reliability of the system. Based on the above considerations and ease of research and analysis, the IEEE 33-node system of the distribution network has been modified appropriately, and nodes 1, 18, 22, 25 and 33 are set as substation access points, as shown in Figure 1.

Preprints (www.preprints.org) | NOT PEER-REVIEWED | Posted: 24 November 2019 doi:10.20944/preprints201911.0280.v1

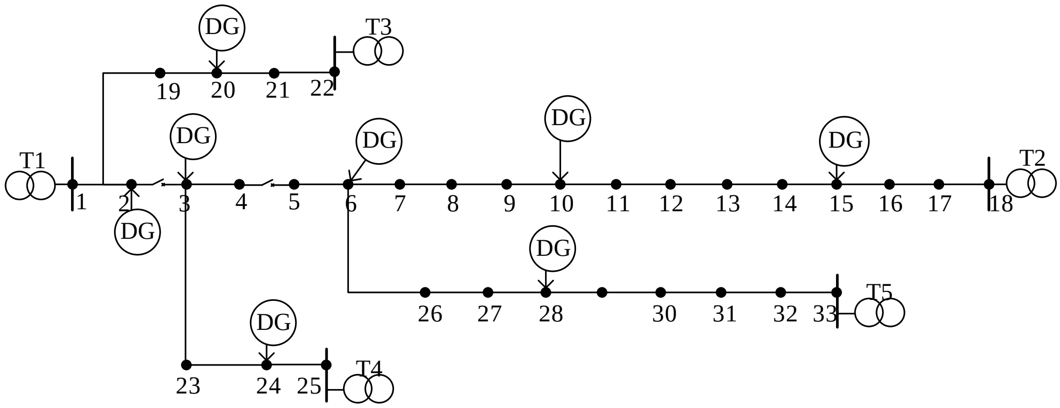

Figure 1. The IEEE 33-bus distribution network

5.1. The Influence of the Node Voltage Allowable Lower Limit and Substation Capacity on TSC

The relationship between TSC substation capacity and TSC is shown in Figure 2. Due to the limitation of the maximum current I_{max} allowed by the line, when the substation capacity reaches a certain value, it has no effect on the promotion of TSC. By observing the curves of three different trends, it can be found that the maximum current allowed by different lines will change the upper limit of the influence of the capacity of the substation. In a certain range of substation capacity, the maximum allowable current change of the line has no effect on the TSC.

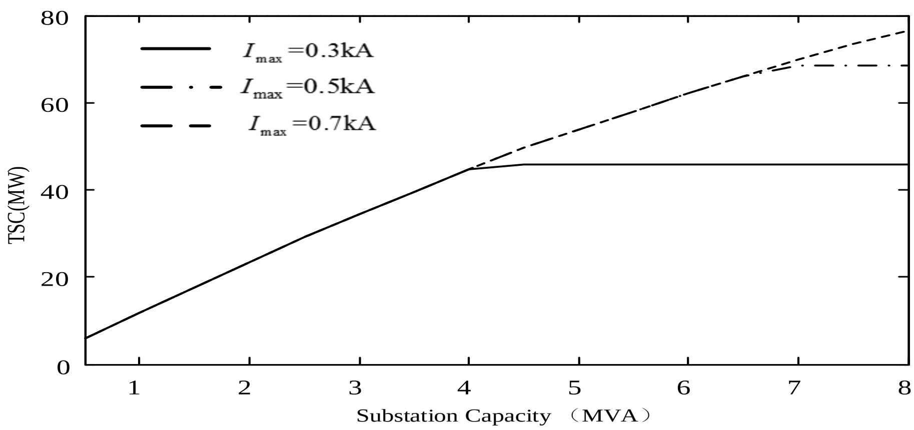

Figure 2. Impact of substation capacity on TSC

The relationship between the switching states of circuit breaker and the node voltage lower limit values is shown in Figure 3.

In Figure 3, the ordinate indicates the node number corresponding to the faulty substation, and the five substations correspond to five bar graphs. When the circuit breaker is closed, the corresponding position in the bar graph is a rectangle. When the circuit breaker is disconnected, the corresponding position in the bar graph is a straight line. Figure 3 is divided into six parts based on the phase and breaker number. Figure 3 shows that all circuit breakers are closed when the lower voltage limit is lower, because the lower voltage lower limit allows the nodal load to obtain the power supply to the farther substation. For example, when line 4-5 is in the connected state, node 5 is able to obtain the power supply to the substation at node 18 and node 33. This effect is more pronounced as the substation capacity is smaller.

Conversely, when the lower voltage limit is higher, the substation has to select a load with a closer distance. At the same time, once the circuit breaker is opened, the voltage relationship between the two ends of the circuit breaker is no longer limited, which further alleviates the hindrance of voltage constraints to the improvement of power supply capacity. Therefore, most of the circuit breakers are in the open state. Taking node 5 as an example, the voltage loss is smaller from node 5 to node 22 and node 25 compared to node 5 to node 18 and node 33, which makes the closure of circuit breaker 1 more advantageous and TSC boost. Similarly, when the substation of node 22 and node 25 fails, the circuit breaker is also in a closed state when the minimum allowable voltage value is large. In summary, when the distribution network responds to changes in the allowable value of the lower voltage limit, the presence of the circuit breaker makes the TSC upgrade more flexible.

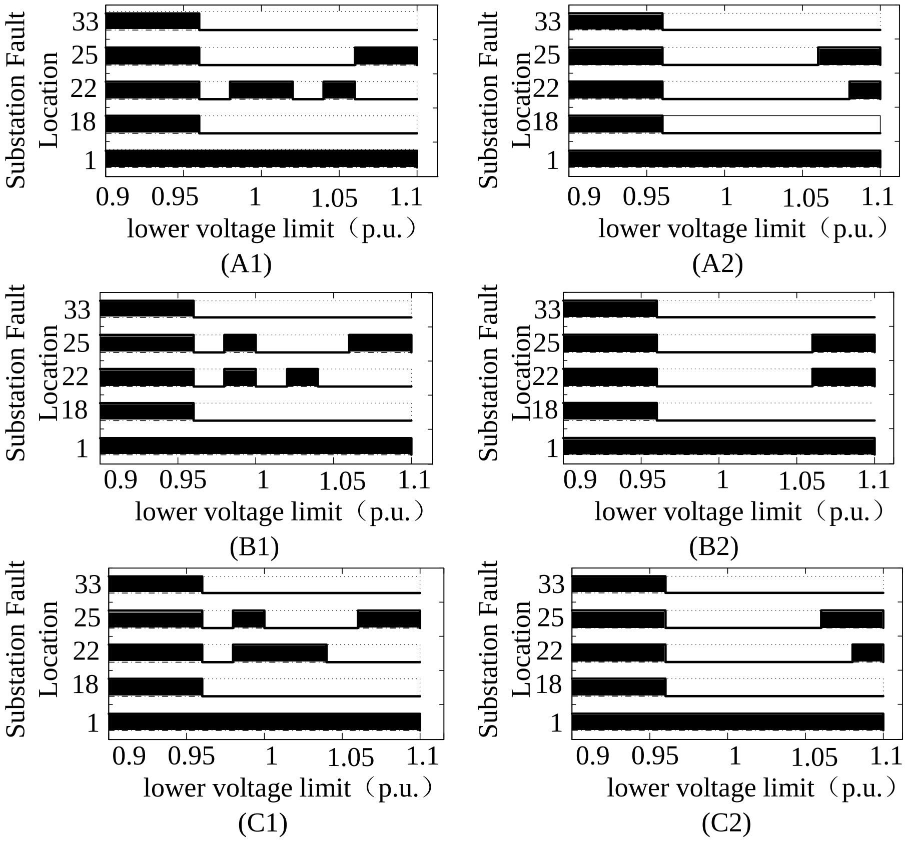

Figure 3. Relationship between voltage lower limit and circuit breaker status

Figure 4 shows the optimization results of the TSC under the constraints of the substation capacity and lower voltage limit. Figure 4 shows that the TSC analysis can provide guidance for the planning and design of substation capacity in the distribution system based on the corresponding voltage constraints in order to make more efficient use of the capacity of the transformer. Figure 4(b) and Figure 4(c) show that as the lower voltage limit increases, the TSC gradually decreases. When the voltage lower limit is below the critical value, the TSC is substantially unaffected.

It should be additionally noted that the higher the voltage lower limit represents the higher the requirement for voltage quality, but it does not mean that the voltage level must be used as a decision variable in the actual planning. In actual situations, it can be decided according to different design requirements.

Preprints (www.preprints.org) | NOT PEER-REVIEWED | Posted: 24 November 2019 doi:10.20944/preprints201911.0280.v1

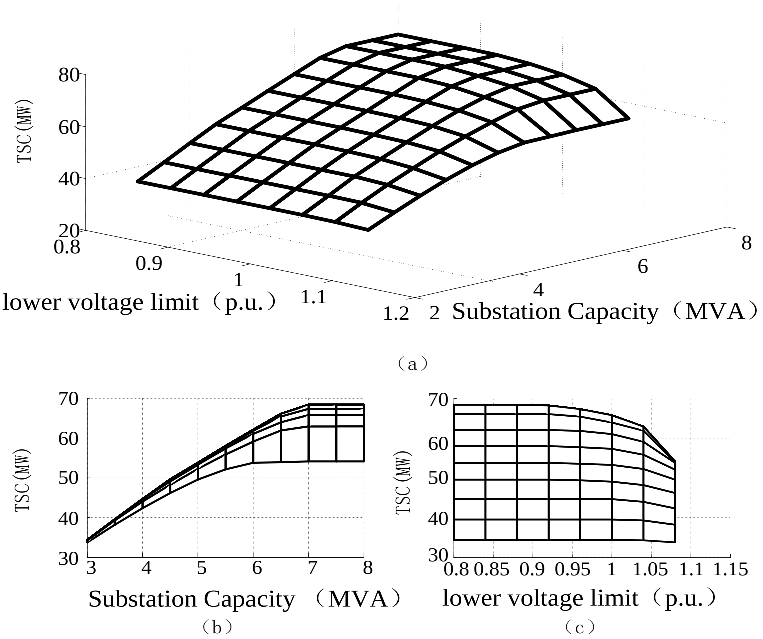

Figure 4. Synergy relationship between TSC and substation capacity and voltage lower limit

5.2. TSC Analysis Taking into Account Single-Phase DG Access

The case of single-phase DG access is considered to highlight the effects of three-phase asymmetry. The relationship between the upper limit of DG output and TSC is shown in Figure 5.

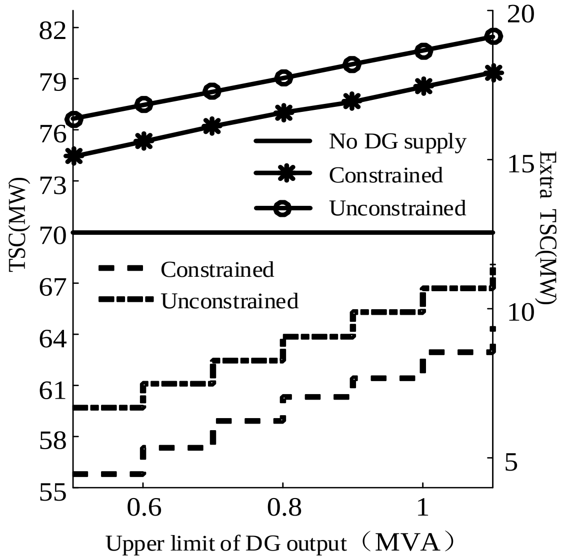

Figure 5. The impact of the upper limit of DG output on TSC

Figure 5 is a double ordinate form that can be divided into two parts. The first part is to evaluate the TSC after a single-phase distributed power access system. The second part shows the TSC benefits of DG, which is shown in the lower part of the figure. Both parts give a comparison of the presence or absence of three-phase unbalance constraints. In order to highlight the asymmetry of the distributed power supply, only the distributed power supply of phase A is considered. Figure 5 shows that after accessing the distributed power supply, the TSC has a significant increase and brings a power supply capability that exceeds the sum of the maximum output of the distributed power supply. This is because the distributed power supply can take advantage of short-distance transmission and make up for the power loss caused by the failure of each substation. It can directly transmit power to users facing the risk of power outage without receiving power from other substations remotely. However, with the increase of the upper limit of DG output, the benefits

Preprints (www.preprints.org) | NOT PEER-REVIEWED | Posted: 24 November 2019 doi:10.20944/preprints201911.0280.v1

brought by DG are no longer obvious, and the growth trend of TSC is basically the same as the increase of the maximum output of DG. This shows that the extra distributed power output will no longer supply power to remote loads, but only increase the power supply potential of the DG access node.

A detailed observation of Fig. 5 reveals that after the addition of the three-phase unbalance constraint, TSC is limited by the asymmetric variation of the three-phase current distribution caused by the access of the single-phase distributed power source. With the upper limit of DG output, the growth trend of TSC considering the three-phase unbalance constraint is roughly the same as that without considering the constraint. This is because the remaining distributed power output is limited by the imbalance constraints, making it impossible to supply load of remote nodes through the line transmission. Eventually, only the load on the access node can be selected for supply.

Assuming that there are only eight alternative DG access nodes, the simulation results shown in Figure 6 are obtained by controlling the number of access points of the distributed power supply, wherein the maximum output of each distributed power supply is 1 MVA.

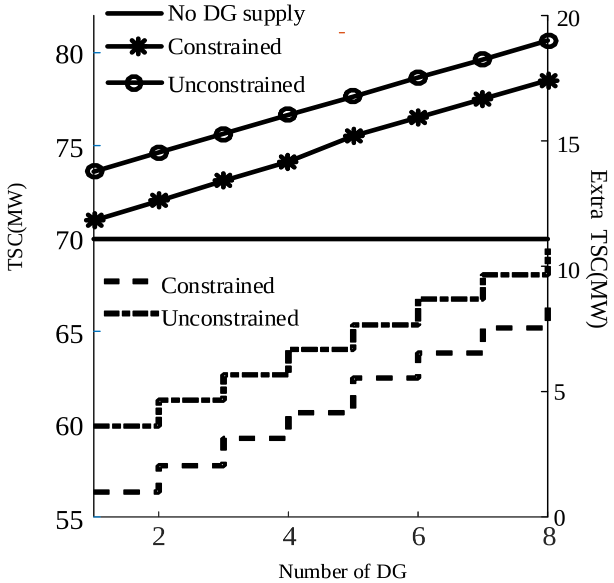

Figure 6. The impact of the upper limit of DG on TSC

The relationship between the upper limit of the number of DGs and the average output of DG is shown in Fig. 7. The ordinate of Figure 7 represents the average power supply benefit from each distributed power source. This benefit is obtained by the relationship between the extra TSC and the number of DGs.

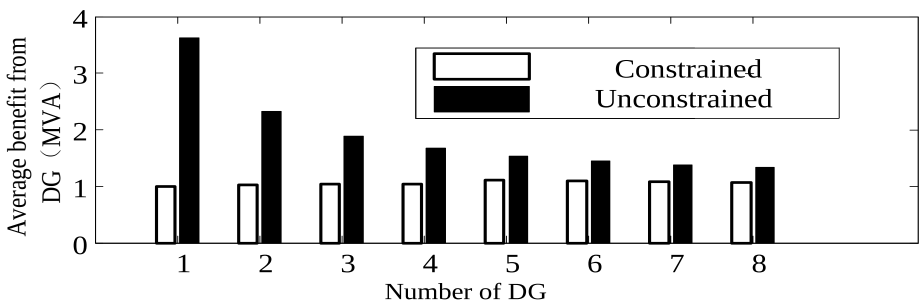

Figure 7. The relationship between the upper limit of DG quantity and the average output of DG

Figures 6 and 7 show that, in particular, when the three-phase unbalance constraint is not taken into account, the distributed power source brings the power supply capability to a quantity that exceeds its own maximum output sum. The power supply capacity gain of the station is also gradually reduced as the number of DG units increases. In the power grid structure, the distributed

Preprints (www.preprints.org) | NOT PEER-REVIEWED | Posted: 24 November 2019 doi:10.20944/preprints201911.0280.v1

power flow distribution of some distributed power sources overlaps, so that in the case of partial faults, these distributed power supplies maintain lower power output in order to avoid line power crossing. In addition, after accounting for the three-phase unbalance constraint, the average power supply capability gain from the distributed power supply is roughly equal to the upper limit of the distributed power output. Since the optimization trend of the model is to obtain more power supply capability, the DG output that cannot flow have to be absorbed locally.

The relationship between three-phase unbalance and TSC is shown in Figure 8. Figure 8 shows that as the allowable value of the three-phase unbalance is increased, the TSC gradually rises and the rising trend is slower. Combined with the analysis of Figure 6 and Figure 7, it can be seen that because the DG is limited by the three-phase unbalance degree, it can more flexibly compensate for the power failure loss caused by the distribution network failure.

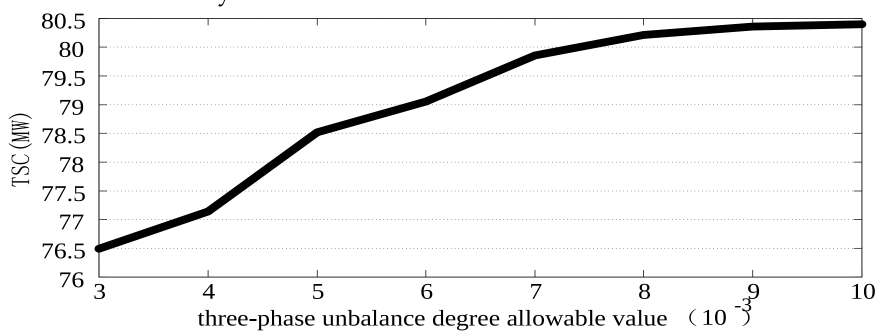

Figure 8. TSC and three-phase unbalance degree allowable value relationship diagram

5.3. TSC Analysis Taking Into Account Load Response

For the sake of analysis, only the distribution network of phase A is studied. The distribution of load output at each point of phase A is shown in Figure 9.

The histogram in Fig. 9 shows the load distribution of each node, the white column indicates the load distribution after considering the load response, and the black portion indicates the load distribution without considering the load response, where nodes 7, 8, 29, 30 and 31 are controllable load node. When the load demand of the controllable load nodes is reduced, the power supply of some nodes is greatly improved, and the overall power supply capacity in phase A is increased from 21.8 MVA to 22.1 MVA. This shows that the power distribution system can improve the power supply capability of some nodes and the overall network through load shedding under the premise of meeting security constraints.

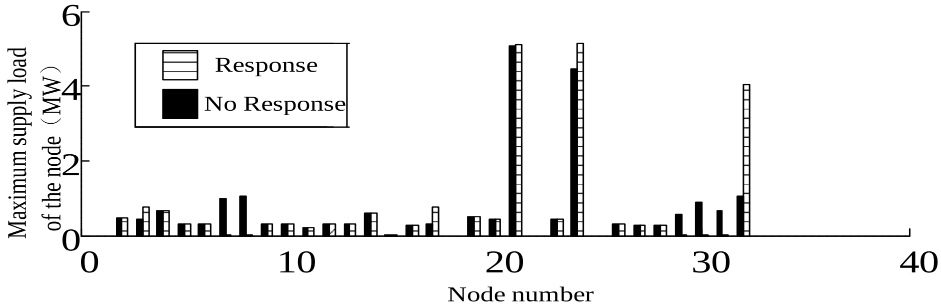

Figure 9. Distribution of load output of each node in phase A

5.4. The Influence of the Proportional Coefficient on TSC and the Verification of the Accuracy of the SOCP

Figure 10 shows that as the coefficient increases, the TSC and system network losses decrease. The simulation results show a higher level of network loss compared to the method of [21]. This is because the load distribution in the literature [21] is mostly at the front end of the network and does not require long-distance transmission of power. However, in order to meet the load requirements of each node in this paper, the supply of power has to be transmitted by long-distance lines, which

Preprints (www.preprints.org) | NOT PEER-REVIEWED | Posted: 24 November 2019 doi:10.20944/preprints201911.0280.v1

results in an undesired network loss. Figure 10 provides guidance recommendations that help to trade off between choosing a larger TSC and a smaller network loss.

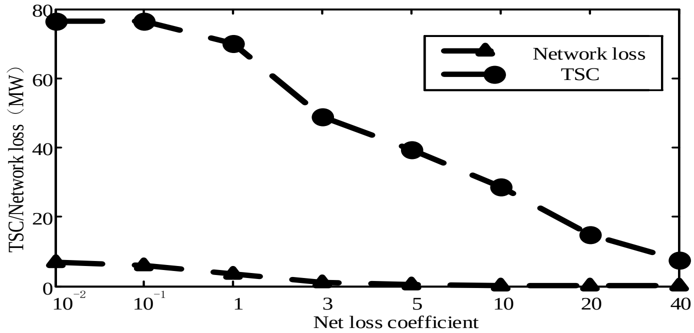

Figure 10. Network loss coefficient and relationship between TSC and network loss

5.5. TSC Result Compared with Other Method

The infinite norm of the second-order cone relaxation error vector defining the branch is as follows [16]:

$$\mathrm{Gap} = \left\| (I_{ij}^{\varphi})^2 - \frac{(P_{ij}^{\varphi})^2 + (Q_{ij}^{\varphi})^2}{(V_i^{\varphi})^2} \right\|_{\infty} \tag{41}$$

Figure 11 shows that as the network loss coefficient increases, the line average current and second-order cone error of the system gradually decrease. This shows that by controlling the objective function, the error of the second-order cone relaxation can be effectively adjusted.

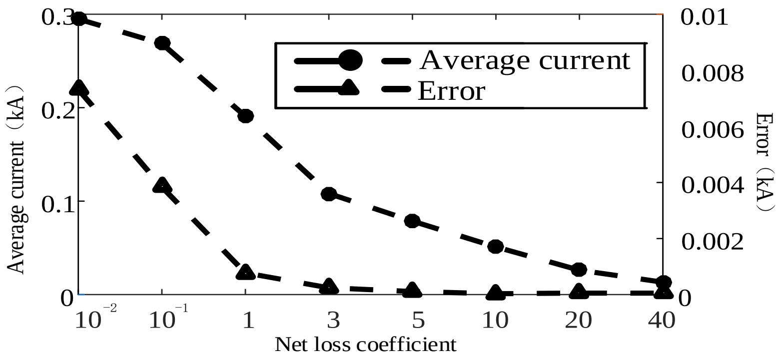

Figure 11. Network loss coefficient and average current and error relationship

Establish a network model as shown in Figure 12 according to the method in [2]. The TSC obtained by this method is 105 MVA, and the result is significantly larger than the calculated result when the power flow distribution is taken, and exceeds the sum of the capacities of all the transformers. This result indicates that the node voltage, branch current, and three-phase unbalance constraints all have critical limitations on TSC.

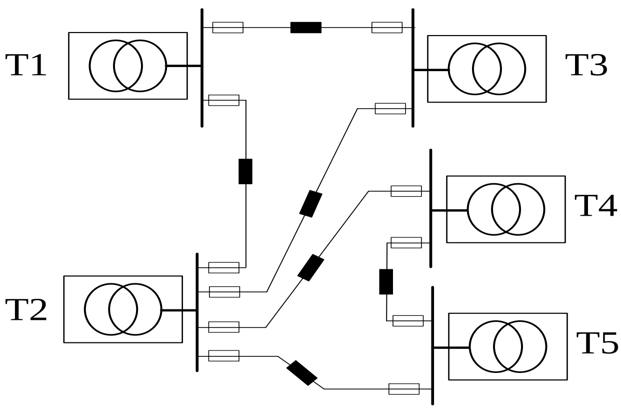

Figure 12. Schematic diagram

 doi:10.20944/preprints201911.0280.v1

5. Conclusions

1. Compared with previous studies, this paper incorporates the three-phase power flow model into the calculation of maximum power supply capacity. The three-phase power flow calculation model can complete the "N-1" check on the basis of satisfying the certain three-phase unbalance of each phase. Considering the asymmetric distributed power output and load demand, the impact of substation capacity, voltage limit and DG parameters on TSC is more comprehensively evaluated, which provides more reference for the planning of distribution network.
2. The circuit breaker and load response enable the distribution network architecture to flexibly upgrade the TSC, enabling the distribution network to meet load demands in complex fault conditions.
3. The results of the maximum power supply calculation meet the accuracy requirements. After the second-order cone relaxation, the power flow error range is within the allowable range, and the optimal solution is the critical point on the main transformer "N-1" safety boundary, which satisfies the power flow constraint condition.

Author Contributions: Conceptualization and methodology, J.Z.; formal analysis, J.Z.; investigation, S.N.; resources, P.S.; software, G.W.; validation, P.S.; writing—original draft preparation, J.Y.; writing—review and editing, R.W.; visualization, C.Y.; supervision, Z.H.

Funding: This research was funded by National Natural Science Foundation of China (No. 51977156).

Conflicts of Interest: The authors declare no conflict of interest.

Appendix A

Suppose the three-phase voltages of a node are V_{av}, V_{bv} and V_{cv}, respectively, and there must be a maximum value, a minimum value, and an intermediate value. According to the definition of the three-phase unbalance degree, formula (A1) and formula (A2) are defined, and V_t refers to the three-phase unbalance factor.

$$V_t = \max\left(\left|\frac{V_{min} - V_{av}}{V_{av}}\right|, \left|\frac{V_m - V_{av}}{V_{av}}\right|, \left|\frac{V_{max} - V_{av}}{V_{av}}\right|\right) \tag{A1}$$

$$V_{av} = \frac{V_{min} + V_m + V_{max}}{3} \tag{A2}$$

According to formula (A1), the relationship between the variables can be known:

$$V_t = \max\left(\left|\frac{V_{min} - V_{av}}{V_{av}}\right|, \left|\frac{V_{max} - V_{av}}{V_{av}}\right|\right) \tag{A3}$$

$$\left|\frac{V_{min} - V_{av}}{V_{av}}\right| = \left|\frac{3V_{min}}{V_{min} + V_m + V_{max}} - 1\right| = \left|\frac{3}{1 + \frac{V_m}{V_{min}} + \frac{V_{max}}{V_{min}}} - 1\right| \tag{A4}$$

$$\left|\frac{V_{max} - V_{av}}{V_{av}}\right| = \left|\frac{3V_{max}}{V_{min} + V_m + V_{max}} - 1\right| = \left|\frac{3}{\frac{V_{min}}{V_{max}} + \frac{V_m}{V_{max}} + 1} - 1\right| \tag{A5}$$

$$(1 + \frac{V_m}{V_{min}} + \frac{V_{max}}{V_{min}}) \geq 3 \tag{A6}$$

$$1 < (\frac{V_{min}}{V_{max}} + \frac{V_m}{V_{max}} + 1) \leq 3 \tag{A7}$$

When the voltage is squared, the following formulae can be derived according to the above formulae:

$$V_t^2 = \max\left(\left| \frac{V_{\min}^2 - V_{av}^2}{V_{av}^2} \right|, \left| \frac{V_{\max}^2 - V_{av}^2}{V_{av}^2} \right| \right) \quad \text{(A8)}$$

$$V_{av}^2 = \frac{V_{\min}^2 + V_{\mathrm{m}}^2 + V_{\max}^2}{3} \quad \text{(A9)}$$

$$\left| \frac{V_{\min}^2 - V_{av}^2}{V_{av}^2} \right| = \left| \frac{3V_{\min}^2}{V_{\min}^2 + V_{\mathrm{m}}^2 + V_{\max}^2} - 1 \right| = \left| \frac{3}{1 + \frac{V_{\mathrm{m}}^2}{V_{\min}^2} + \frac{V_{\max}^2}{V_{\min}^2}} - 1 \right| \quad \text{(A10)}$$

$$\left| \frac{V_{\max}^2 - V_{av}^2}{V_{av}^2} \right| = \left| \frac{3V_{\max}^2}{V_{\min}^2 + V_{\mathrm{m}}^2 + V_{\max}^2} - 1 \right| = \left| \frac{3}{\frac{V_{\min}^2}{V_{\max}^2} + \frac{V_{\mathrm{m}}^2}{V_{\max}^2} + 1} - 1 \right| \quad \text{(A11)}$$

According to the relationship between $\frac{V_{\max}^2}{V_{\min}^2} \geq \frac{V_{\max}}{V_{\min}}$ and $\frac{V_{\max}^2}{V_{\min}^2} \leq \frac{V_{\max}}{V_{\min}}$, the following formulae can be derived:

$$(1 + \frac{V_{\mathrm{m}}^2}{V_{\min}^2} + \frac{V_{\max}^2}{V_{\min}^2}) \geq (1 + \frac{V_{\mathrm{m}}}{V_{\min}} + \frac{V_{\max}}{V_{\min}}) \geq 3 \quad \text{(A12)}$$

$$(\frac{V_{\min}^2}{V_{\max}^2} + \frac{V_{\mathrm{m}}^2}{V_{\max}^2} + 1) \leq (\frac{V_{\min}}{V_{\max}} + \frac{V_{\mathrm{m}}}{V_{\max}} + 1) \leq 3 \quad \text{(A13)}$$

According to (A4), (A5), (A10) - (A13), the following formulae can be derived:

$$\left| \frac{V_{\min} - V_{\mathrm{av}}}{V_{\mathrm{av}}} \right| \leq \left| \frac{V_{\min}^2 - V_{av}^2}{V_{av}^2} \right| \quad \text{(A14)}$$

$$\left| \frac{V_{\max} - V_{av}}{V_{av}} \right| \leq \left| \frac{V_{\max}^2 - V_{av}^2}{V_{av}^2} \right| \quad \text{(A15)}$$

Finally we can draw conclusions:

$$V_t^2 \geq V_t \quad \text{(A16)}$$

It can be seen from the above derivation that the voltage imbalance expressed by the quadratic term satisfies the constraint condition, and the originally defined voltage imbalance degree certainly satisfies the constraint condition.

References

1. Sun, W.; Zhang, J. Probabilistic Evaluation and Improvement Measures of Power Supply Capability Considering Massive EV Integration. *Electronics* **2019**, *8*, 1158.
2. Xiao, J.; Li F. Total supply capability and its extended indices for distribution systems: definition, model calculation and applications. *IET Generation Transmission & Distribution* **2011**, *5*, 869-876.
3. Miu, K.N.; Chiang, H.D. Electric distribution system load capability: problem formulation, solution algorithm, and numerical results. *IEEE Transactions on Power Delivery* **2000**, *15*, 436-442.
4. Chen, K.; Wu, W. A Method to Evaluate Total Supply Capability of Distribution Systems Considering Network Reconfiguration and Daily Load Curves. *IEEE Transactions on Power Systems* **2016**, *31*, 2096-2104.
5. Luo, F.; Wang, C. Rapid evaluation method for power supply capability of urban distribution system based on N-1 contingency analysis of main transformers. *International Journal of Electrical Power & energy Systems* **2010**, *32*, 1063-1068.
6. Ge, S.; Han, J. Power supply capability determination considering constraints of transformer overloading and tie-line capacity. *Proceedings of the CSEE* **2011**, *31*, 97-103.
7. Xiao, J.; Liu, S. Model of total supply capability for distribution network based on power flow calculation. *Proceedings of the CSEE* **2014**, *34*, 5516-5524.
8. Zou, K.; Agalgaonkar, A. P. Distribution System Planning with Incorporating DG Reactive Capability and System Uncertainties. *IEEE Transactions on Sustainable Energy* **2012**, *3*, 112-123.

9. Xie, S.; Hu, Z. Multi-objective active distribution networks expansion planning by scenario-based stochastic programming considering uncertain and random weight of network. *Applied Energy* **2018**, *219*, 207-225.
10. Borges, C.; Martins, V. Active distribution network integrated planning incorporating distributed generation and load response uncertainties. 2012 IEEE Power and Energy Society General Meeting, San Diego, CA, 2012.
11. Wang, Y.; Xu, W. The existence of multiple power flow solutions in unbalanced three-phase circuits. *IEEE Transactions on Power Systems* **2003**, *18*, 605-610.
12. Garces, A. A Linear Three-Phase Load Flow for Power Distribution Systems. *IEEE Transactions on Power Systems* **2016**, *31*, 827-828.
13. Wang, Y.; Zhang, N. Linear three-phase power flow for unbalanced active distribution networks with PV nodes. *CSEE Journal of Power and Energy Systems* **2017**, *3*, 321-324.
14. Ding, T.; Li, F. Interval radial power flow using extended DistFlow formulation and Krawczyk iteration method with sparse approximate inverse preconditioner. *IET Generation, Transmission & Distribution* **2015**, *9*, 1998-2006.
15. Gupta A.; Swathika O.V.G.; Hemamalini, S. Optimum Coordination of Overcurrent Relays in Distribution Systems Using Big-M and Dual Simplex Methods. 2015 International Conference on Computational Intelligence and Communication Networks (CICN), Jabalpur, 2015.
16. Liu, Y.; Wu, W. Reactive power optimization for three-phase distribution networks with distributed generators based on mixed integer second-order cone programming. *Automation of Electric Power Systems* **2014**, *38*, 58-64.
17. Smith, J.C.; Hensley, G.; Ray, L. IEEE recommended practice for monitoring electric power quality. IEEE Std. 1159-1995. New York, 1995.
18. Xue, F. Unbalanced three-phase distribution system power flow with distributed generation using affine arithmetic. 2015 5th International Conference on Electric Utility Deregulation and Restructuring and Power Technologies (DRPT), Changsha, 2015.
19. Ueda , Y.; Kurokawa ,K. Analysis Results of Output Power Loss Due to the Grid Voltage Rise in Grid-Connected Photovoltaic Power Generation Systems. *IEEE Transactions on Industrial Electronics* **2008**, *55*, 2744-2751.
20. Liu, J.; Liu, S. Optimal distributed generation allocation in distribution network based on second order conic relaxation and Big-M method. *Power System Technology* **2018**, *42*, 2604-2611.
21. Che, R.; Li, R. A new three-phase power flow method for weakly meshed distribution systems. *Proceedings of the CSEE*, **2003**, *23*, 74-79.